

EVLA Memo 171

Bandpass Stability: A 59 kHz Ripple

Claire Murray (UW Madison), Miller Goss (NRAO), Snežana Stanimirović (UW Madison)

September 18, 2013

1 Introduction

Our project, 21-SPONGE (“21-cm SPectral Line Observations of Neutral Gas with the (E)VLA”), is a survey of high sensitivity HI absorption lines. We aim to reach RMS noise levels in optical depth of $\Delta\tau \sim 5 \times 10^{-4}$ and after completing the first third of the survey (20/58 sources), our median RMS noise is $\Delta\tau \sim 7 \times 10^{-4}$. This high sensitivity allows us to detect both wide ($\Delta v > 5$ km/s) and narrow ($\Delta v < 3$ km/s) absorption lines with optical depths of $\tau \sim 0.001$ or greater. Our ultimate goal is to measure the temperature and column density distributions of the warm and cold neutral media (WNM and CNM) directly in absorption. Especially in the case of the WNM, absorption lines are very wide and shallow and only a handful of direct detections exist to date. Therefore we require extremely high sensitivity and stable baselines in order to reliably detect these lines.

To achieve such high sensitivity, we require very sensitive bandpass solutions, and typically allocate up to 40 percent of every observation to bandpass calibration overhead. In order to minimize noise levels in bandpass solutions, we have experimented with averaging bandpass observations acquired on different days, spaced in time by up to one week. These solutions demonstrate remarkable stability in time. In the process of investigating this stability, we find that the bandpass solutions contain a sinusoidal “ripple” with a period of 59 kHz (or $\Delta v \sim 12$ km/s at our velocity resolution) and amplitude of ~ 0.0015 . The period, amplitude and phase of this ripple are constant between array configurations and time of year. We are able to successfully model and remove this feature from the absorption line profiles, so that we are able to detect individual lines with widths greater than $\Delta v \sim 1$ km/s and up to ~ 20 km/s. We believe that the ripple is caused by the finite impulse response (FIR) filters applied prior to correlation which are used to shape the bandpass. The filters produce a bandpass ripple in the solution, and although this has not been observed before at this level, this effect is expected and confirmed by the correlator engineering group at NRAO. The constant relative amplitude, phase and period of the ripple can all be explained in this context.

2 Methods

2.1 Observing Setup

For the observations, we use three separate, standard L-band configurations, each with one dual polarization IF of 500 kHz bandwidth covered by 256 channels (at 1.95 kHz per channel). One is centered at 1.420408 GHz (near the HI line rest frequency, standard), one at 1.421908 GHz (1.5 MHz, or about 300 km/s, higher than the HI rest frequency, called high) and one at 1.418908 GHz (1.5 MHz lower, called low). We use the “high” and “low” configurations for observing our

bandpass calibrators in order to avoid the typically strong emission and absorption lines that would contaminate the profiles of the bandpass calibrators at the HI rest frequency. Because we normalize our solution with respect to the continuum level, the absolute phase change associated with this frequency switching method is not an issue. We use the standard configuration for observing target sources and measuring HI absorption.

2.2 Data Reduction

We reduce all data using AIPS. After flagging and initial bandpass calibration of the “high” and “low” frequency offset bandpass observations using BPASS, we use the task BPLOTT to examine the solution from each antenna separately. After calibration, we combine the “high” and “low” observations and re-compute the bandpass solution. We then export the final bandpass table using POSSM for further analysis outside of AIPS.

3 Results

In Figures 1a and 2a we show two examples of the bandpass solutions. We have zoomed in on the central channels so that the structure of the solution is easier to see. In addition to a linear slope in the bandpass solution, we observe a sinusoidal ripple that appears to have a roughly constant period. We also show the absorption profiles observed in the directions of 3C298 and PKS0531, given these bandpass solutions (Figure 1b and 2b). In the bottom panels we zoom in at the top of the profiles to show that the bandpass shape was successfully modeled and the baselines are stable and flat. We include our Gaussian fits to these line profiles to demonstrate that we are able to detect wide, shallow lines, and include relevant parameters in the figure captions.

To investigate the stability of the bandpass ripple itself, we extract bandpass solutions from 23 observations, spanning array configurations and configuration moves between A and C arrays. The observations included were conducted between 03/11 and 07/12. Table 1 contains information about each observation, as well as parameters extracted from fitting the ripple (explained below).

3.1 Fitting Process

In order to estimate the quantitative properties of the ripple, we first fit and remove the linear slope and zoom in on the central channels of the bandpass solution (channels 50-200 out of a total 256). The linear slope does not affect our ability to detect wide absorption lines, and we are only interested in determining the parameters of the ripple and correcting for it.

After removing the linear slope, we apply a narrow filter to the Fourier transform of the bandpass solution to extract the dominant periodic signal within the noise. In Figure 3 we display an example of the results of this process, using the bandpass solution from the PKS0531 observation (Figure 2a). An extended explanation with detailed plots is included in Appendix A.

It is apparent from Figure 3 that the solution is dominated by one periodic component with additional (but much weaker) harmonics. To determine the frequency of the dominant periodic component (and its associated harmonics), we compute a periodogram following the method of Scargle (1982). A periodogram is a decomposition of a signal into a linear combination of periodic functions (here sines and cosines), displayed in the form of power as a function of the frequency of each component. We display the periodograms of all 23 solutions in Figure 4. We normalize them all so that the maximum power per frequency is equal to 1 for easier comparison.

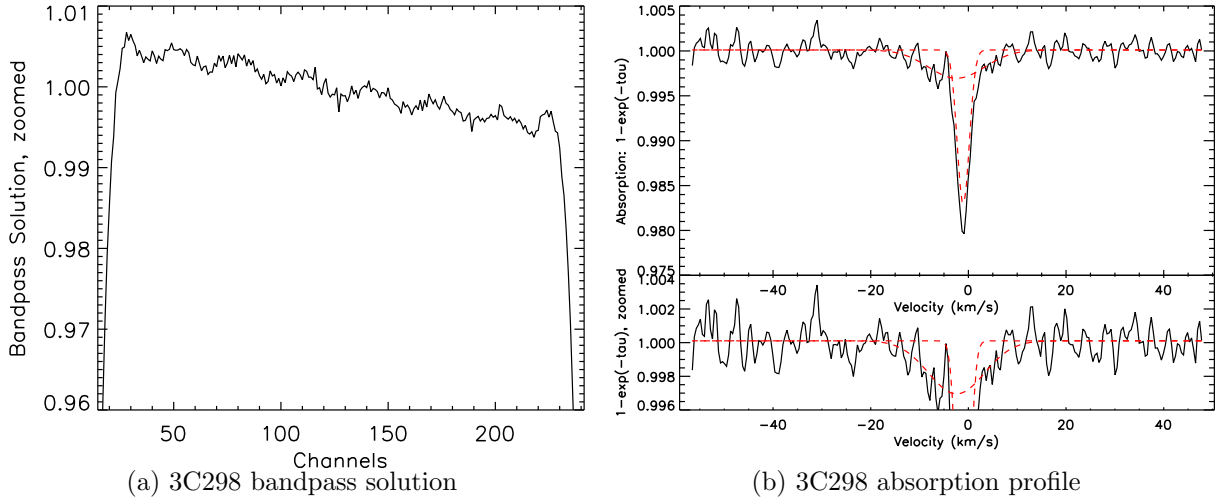


Figure 1: (a): An example bandpass solution, zoomed slightly into the central channels to display the apparent sinusoidal ripple in the solution. This is from the 3C298 observation, see Table 1 for more details. (b): Absorption profile from the target observation (top panel), and a zoom-in on the top of the profile to show that the bandpass ripple was successfully removed. The RMS noise in absorption is $\Delta\tau = 0.0008$. We fit two Gaussian components (red dashed lines), including a wide, shallow component with central velocity $v = -2.4 \pm 0.6$ km/s, width $\Delta v = 13 \pm 2$ km/s and height $\tau = 0.0032 \pm 0.0004$.

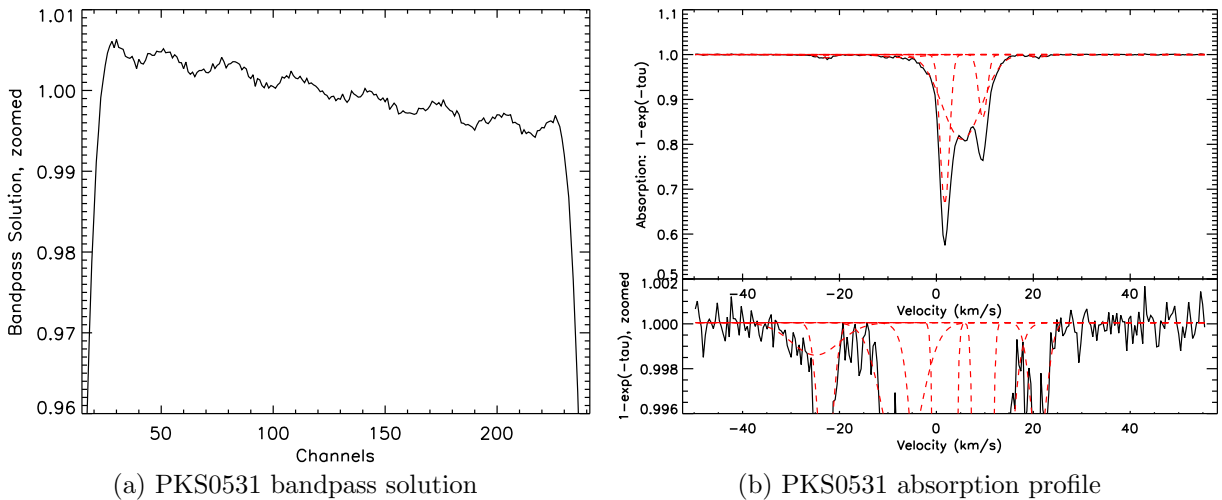


Figure 2: Same as Figure 1 but for a stronger absorption line source, PKS0531. The RMS noise in absorption is $\Delta\tau = 0.0005$. We fit six Gaussian components (red dashed lines), including a shallow component with central velocity $v = -25 \pm 4$ km/s, width $\Delta v = 12 \pm 9$ km/s and height $\tau = 0.0015 \pm 0.001$. The parameters of this component are more uncertain in the presence of a more complex, blended line profile than in Figure 1.

From Figure 4, we can see that all solutions have a dominant component with a period of about 30 channels, and the additional harmonics are weaker by factors between 5 and 10. At our frequency

Table 1: Bandpass Solution Parameters

Information:			Fit Parameters:			
Target Name	Obs. Date	Array Config.	RMS noise ¹ (per channel)	Amplitude ²	Period ² (channels)	Phase ³ (channel)
3C120D1	03/11	B	0.00049	0.0014	30.1	120
3C120D2	03/11	B	0.00047	0.0014	29.9	120
3C286	05/11	B	0.00064	0.0016	29.9	122
3C225BD1	05/11	BnA	0.00049	0.0015	30.0	121
3C225BD2	05/11	BnA	0.00049	0.0015	30.3	121
3C225BD3	05/11	BnA	0.00042	0.0013	30.1	120
4C12.50	05/11	BnA	0.00048	0.0014	30.0	120
3C345	06/11	BnA-A	0.00074	0.0017	30.1	120
3C298	06/11	BnA-A	0.00057	0.0015	29.8	121
4C32.44D1	05/11	BnA-A	0.00040	0.0014	29.9	122
4C32.44D2	06/11	BnA-A	0.00063	0.0015	29.9	120
4C32.44D3	06/11	BnA-A	0.00057	0.0015	29.8	122
3C48	08/11	A	0.00048	0.0014	30.0	120
4C16.09	09/11	A	0.00037	0.0014	30.0	120
4C16.09.2	09/11	A	0.00031	0.0013	29.9	120
3C133	09/11	A-D	0.00035	0.0014	30.1	120
PKS0531	09/11	A-D	0.00031	0.0013	29.9	120
3C111	04/12	C	0.00042	0.0014	29.9	120
3C154D1	04/12	C	0.00057	0.0017	30.2	122
3C154D2	04/12	C	0.00033	0.0013	29.9	120
3C123	05/12	CnB	0.00041	0.0015	30.1	120
3C138	05/12	CnB	0.00041	0.0014	29.9	122
3C410	07/12	B	0.00057	0.0016	29.6	123

¹: the RMS noise calculated in the residuals of the bandpass solution *after* removing the ripple model.

²: calculated using the periodogram analysis of the solution (i.e. these are the parameters of the dominant component)

³: the location of the start of a new sine period close to the center of the solution.

resolution of 1.95 kHz per channel, 30 channels corresponds to about 59 kHz. The amplitude and period extracted from each solution are listed in Table 1, as well as the phase of the solution (calculated as the channel location of the start of a new sine period close to the center). The rms noise values listed in Table 1 are calculated from the residuals of the fit in Figure 3 (see Appendix A, Figure 7a).

From Table 1 we conclude that the amplitude, period and phase of the ripple are stable between all currently tested observations.

3.2 Function of Antenna?

To test if the presence of the ripple is a function of particular antennas, we separated the bandpass solutions into three groups of about 9 antennas (i.e antennas 1-9, 10-18, 19-28). After fitting the solutions from these antenna subsets, we find that the ripple exists at a similar power as in the full solution in all cases. Therefore, we conclude that the effect is not antenna-based.

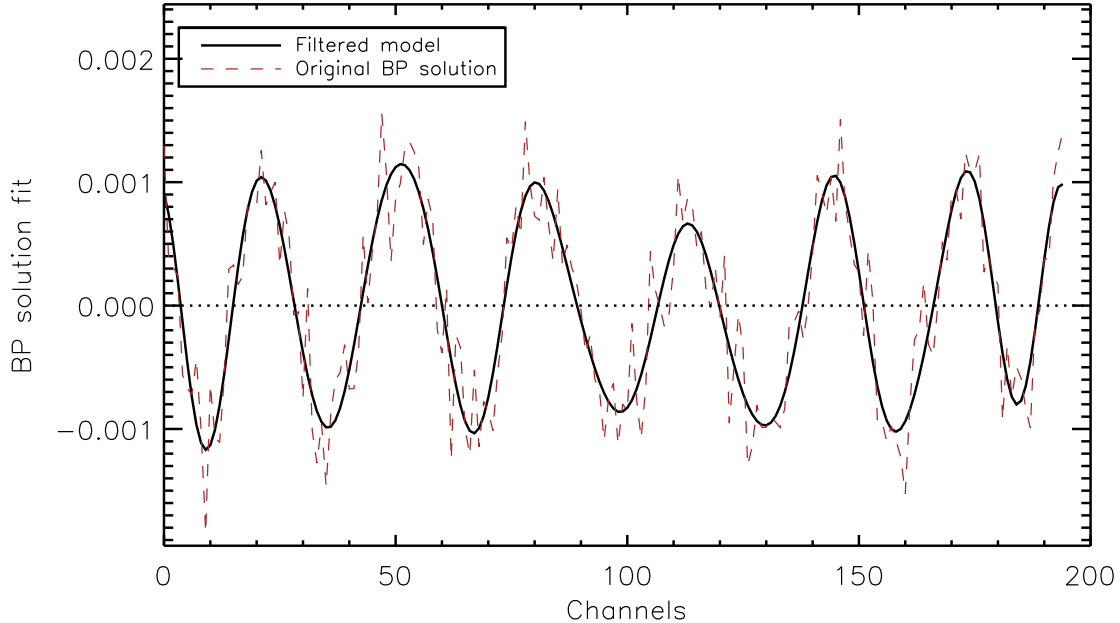


Figure 3: The original bandpass solution from the PKS0531 observation (Figure 2) with linear slope removed (red dashed). The Fourier-filtered fit (see text and Appendix A) is overlaid (solid black).

4 Time Averaging

In addition, we test the method of combining bandpass observation data between separate observations, spaced in time by hours, days and weeks. This is another test of the stability of the bandpass solution. We find that combining observations improves the noise level in the bandpass solution, although not by the theoretically expected amount (i.e. by the square root of the increase in total time). In the future, we plan to investigate this further by combining bandpass solutions after removing a model of the ripple.

In Figure 5 we show an example of this method in the form of the bandpass solution before and after combining observations. All relevant information about the separate observations are included in Table 2 along with additional information about several additional tests. We note the RMS noise values in Table 2 are higher than in Table 1 because they were calculated using ranges of channels in the bandpass solution *before* removing the fit to the periodic component or ripple. However, we are interested in the improvement in the noise level compared with theoretical expectations, so its absolute value is not as important for this particular argument. The noise levels improve consistently by values between 70 and 90 percent of the theoretically expected improvement.

5 Conclusions

We conclude that there is a 59-kHz ripple present in all bandpass solutions from our observations, and this ripple is stable in amplitude, phase and period over time and between configurations. Given the properties we derive here, we conclude that it is an effect caused by the application of finite impulse response (FIR) filters prior to correlation. The filters introduce a bandpass ripple in the solution. This effect is expected and confirmed by the correlator engineering group at NRAO, and

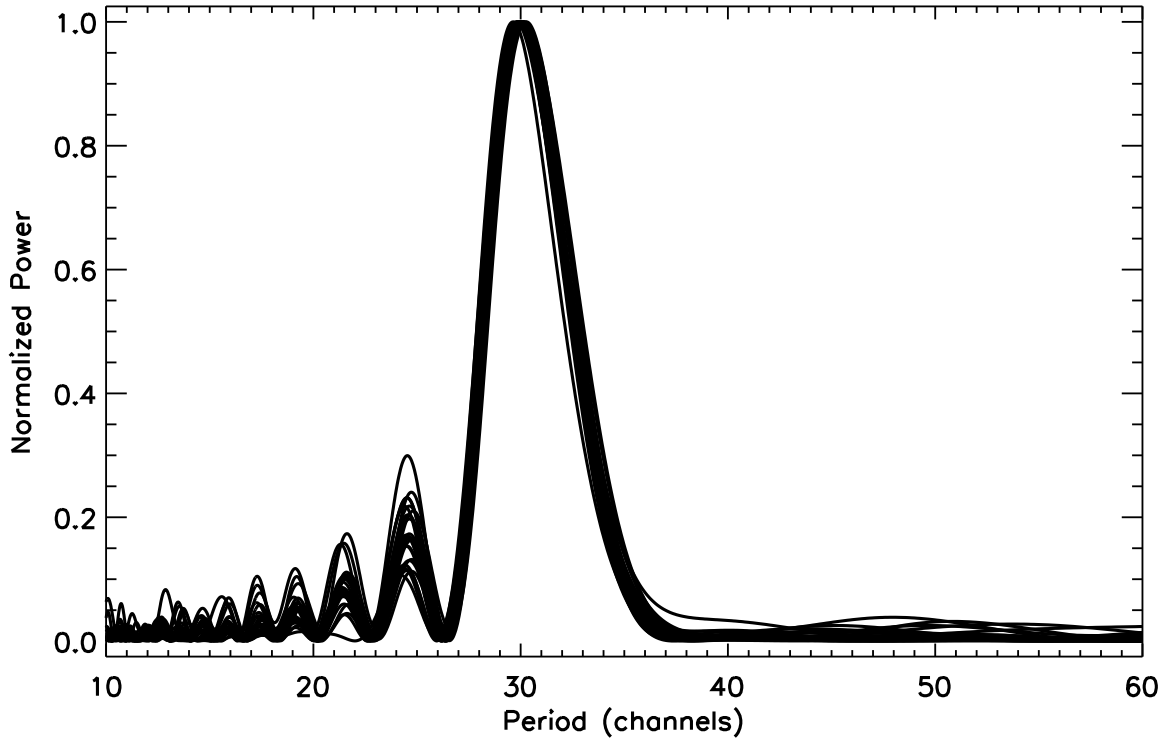


Figure 4: Periodogram results for all 23 solutions plotted together, normalized to 1 for easier comparison.

this is the first time it has been observed at this level. The constant relative amplitude, phase and period can all be explained in this context.

Furthermore, we have found that bandpass solutions are stable in time and can be combined to improve the solution over time periods between hours and many days. Although the improvements to the noise in the bandpass solution do not quite follow theoretical expectations based on the increase in total observing time, the noise does improve in all cases we have tested so far. It will be instructive to test this further and determine the maximum amount of time between observations that this method will work for.

References

Scargle, J.D., 1982, *ApJ*, v.263, p.835.

A Fourier Filtering Analysis

After removing the linear slope from the bandpass solution from the PKS0531 observation (see Figure 2), we isolate the central 200 channels to avoid the bandpass edges. See Figure 3 (or Figure 6b) for an example of the results of this simple process, shown by the dashed red line.

We then compute the Fourier transform (FT) spectrum of this flattened, zoomed solution (see

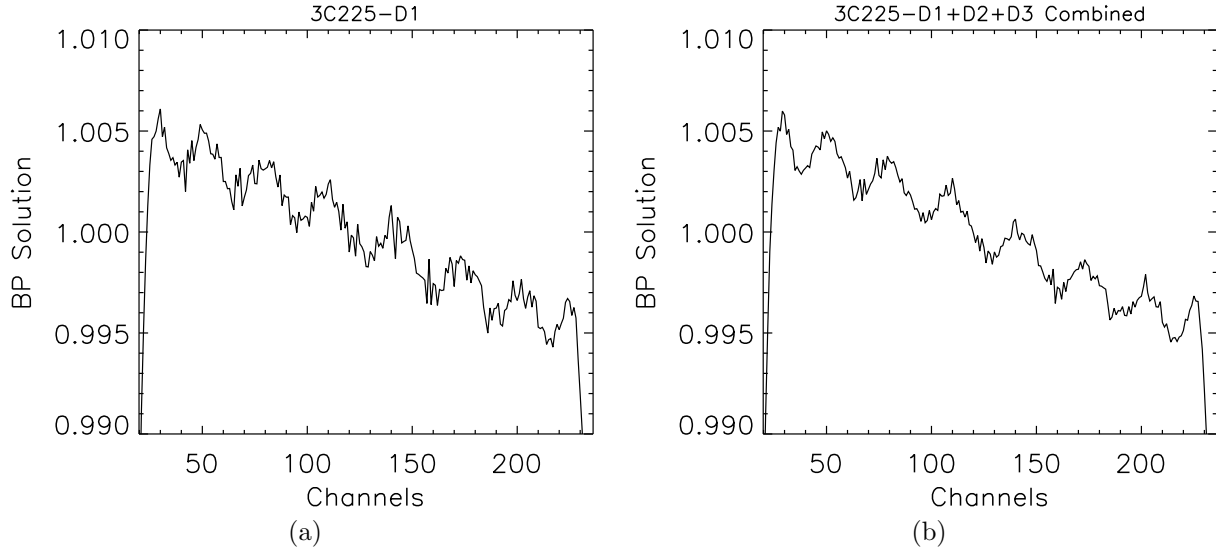


Figure 5: (a): bandpass solution for 3C225-D1 (day one of a series of three observations), computed from 33.4 minutes of observation time. (b): bandpass solution from 3C225-D1 plus two additional days of observation, comprising 103.5 minutes total. The noise level decreases by a factor of 1.3, although not by the theoretically predicted amount of $\sqrt{103.5/33.4} \sim 1.8$. See Table 1 for more details about these and other observations.

Table 2: Time averaging of bandpass solutions

Target Name	BP Name	Obs. Date	RMS in BP ¹	Obs. time (min)	Theor. Imprvmnt ²	Actual Imprvmnt ³	Imprvmnt Ratio ⁴
3C123	3C147	05/16/12+05/18/12	0.0010	88.6	1.4	1.1	0.8
3C138	3C147	05/19/12+05/20/12	0.0011	85.9	1.4	1.2	0.9
All	"	"	0.0009	174.5			
3C410	3C410	07/08/12	0.0022	80	1.4	1.1	0.8
3C454.3	3C454.3	07/08/12	0.0016	84	1.4	1.2	0.9
All	"	"	0.0016	164			
3C225D1	3C147	05/13/12	0.0013	33.4	1.8	1.3	0.7
3C225D2	3C147	05/17/12	0.0012	30.2	1.8	1.2	0.7
3C225D3	3C147	05/20/12	0.0011	39.9	1.6	1.1	0.7
All	"	"	0.0010	103.5			
4C32.44D1	3C286	05/22/11	0.0011	30.8	1.5	1.1	0.7
4C32.44D2	3C286	06/03/11	0.0012	41.1	1.3	1.2	0.9
All	"	"	0.0010	71.9			

¹: calculated over a range of channels in the bandpass solution before removing the fit to the ripple.

²: theoretical improvement to noise level based on additional obs time, Δt (i.e. by $\sqrt{\Delta t}$).

³: actual improvement to noise level based on additional obs time.

⁴: ratio of actual/theoretical improvement

Figure 6a). Next, we multiply this FT spectrum with a simple step function filter to isolate the dominant periodic components. The boundaries of the filter are shown in Figure 6a as vertical dashed lines. We then compute the inverse FT of the filter-multiplied FT spectrum (displayed as

the thick black line in Figure 6a) to model the periodic component. These results are displayed in Figure 6b, as well as in Figure 3 by the solid black line.

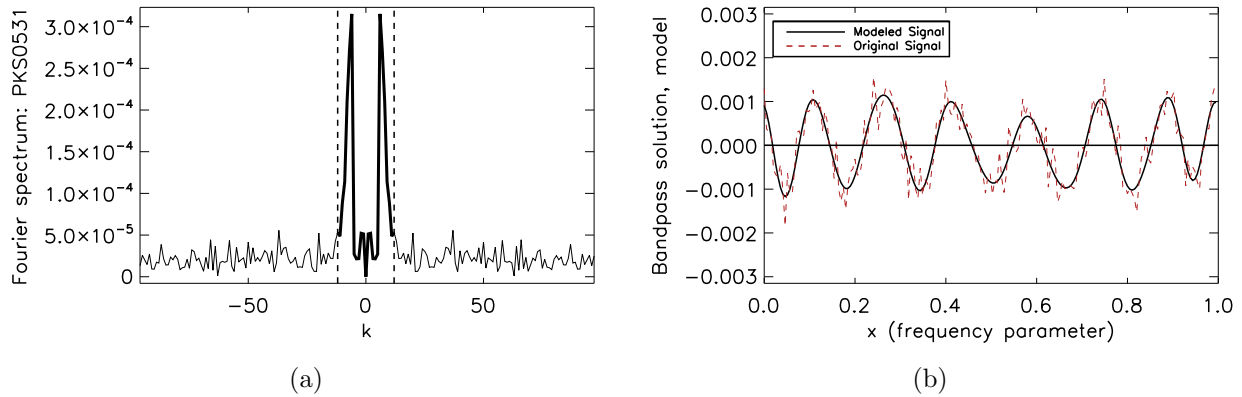


Figure 6: (a): FT spectrum of the bandpass solution from the PKS0531 observation (see Figure 2), with the boundaries of the applied step-function filter overlaid as dashed lines. (b): Model of the bandpass solution (solid black), computed as the inverse FT of the filter-convolved FT spectrum of the bandpass solution. The bandpass solution is overlaid as the dashed red line. “x” is a normalized channel (or frequency) parameter, used to simplify the calculation.

As a test of the success of this model, we compute the residuals by subtracting the model from the bandpass solution (see Figure 7a). We then compute a simple histogram of these residuals in order to observe if they are well-represented by a Gaussian distribution, which we expect if the model is reasonable (see Figure 7b). From this, we can conclude that the model does a reasonably good job of isolating the dominant periodic components of the bandpass solution. We compute the rms noise in these residuals as an indicator of the noise level in the bandpass solution that is not due to the periodic components. These values for all solutions are listed in Table 1.

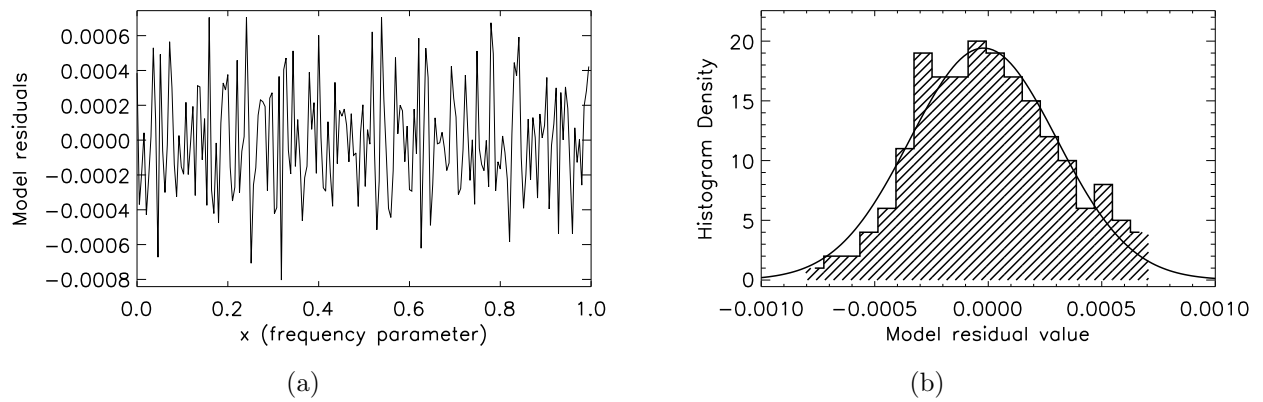


Figure 7: (a): Residuals of the FT model to the bandpass solution displayed in Figure 6 (i.e., bandpass solution minus model). “x” is a normalized channel (or frequency) parameter, used to simplify the calculation. (b): Histogram of the residuals to check if they are well-represented by a Gaussian distribution, as would be expected in the case of a successful model. A Gaussian model is overlaid (solid black line) to illustrate this.